Supporting Information

En Route to Chiral-at-Metal Ruthenium Complexes Containing Tripodal Tetradentate Ligands

Juan Téllez, Isabel Méndez, Fernando Viguri,* Ricardo Rodríguez,* Fernando J. Lahoz, Pilar García-Orduña, and Daniel Carmona*

Instituto de Síntesis Química y Catálisis Homogénea (ISQCH), CSIC - Universidad de Zaragoza, Departamento de Química Inorgánica, Pedro Cerbuna 12, E-50009 Zaragoza, Spain

E-mail: dcarmona@unizar.es (D. C.), riromar@unizar.es, (R. R.), fviguri@unizar.es (F. V.)

Table of Contents

1. Kinetic studies for the isomerization of complex 10a

Eyring equation:
$\ln(k/T) = (-\Delta H^{\neq}/R) \times (1/T) + \ln(k_B/h) + (\Delta S^{\neq}/R)$

[**10a**] = 23.54 mM; solvent = CD_3OD

T (K)	k (s^{-1})	ln (k/T)	1/T
183	431,3904	0,857527328	0,005464481
213	380,3526	0,579806552	0,004694836
233	349,2948	0,404877811	0,004291845
243	332,4672	0,313479765	0,004115226
256	310,689	0,193614967	0,00390625

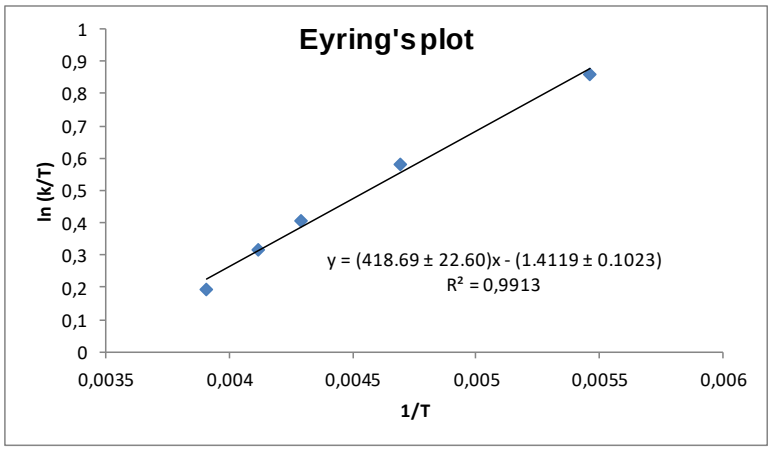

$\Delta G^{\neq} = 12.19 \pm 1.75$ Kcal/mol

$\Delta H^{\neq} = -0.83 \pm 0.02$ Kcal/mol

$\Delta S^{\neq} = -44.4 \pm 5.8$ cal/mol

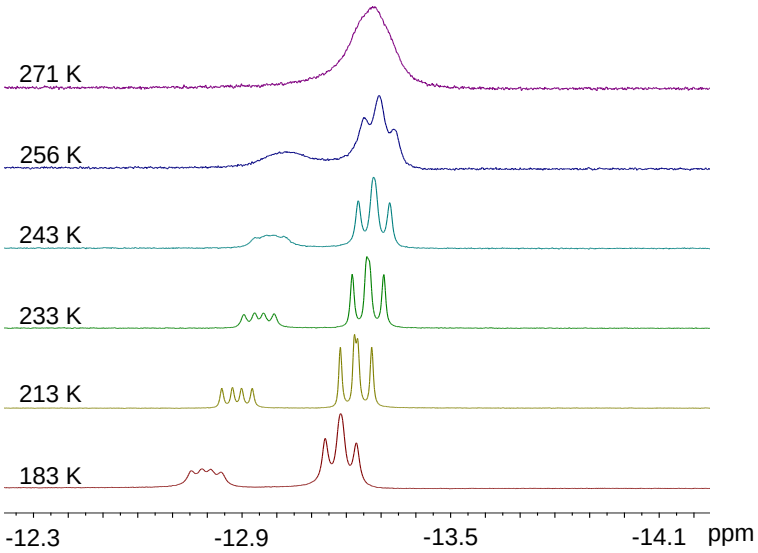

Figure SI1. Kinetic studies for the isomerization of complex **10a**

2. Selected NMR spectra of compound 11-13

Figure SI2. ^{1}H NMR (500.13 MHz, CD_2Cl_2, RT) of **11**

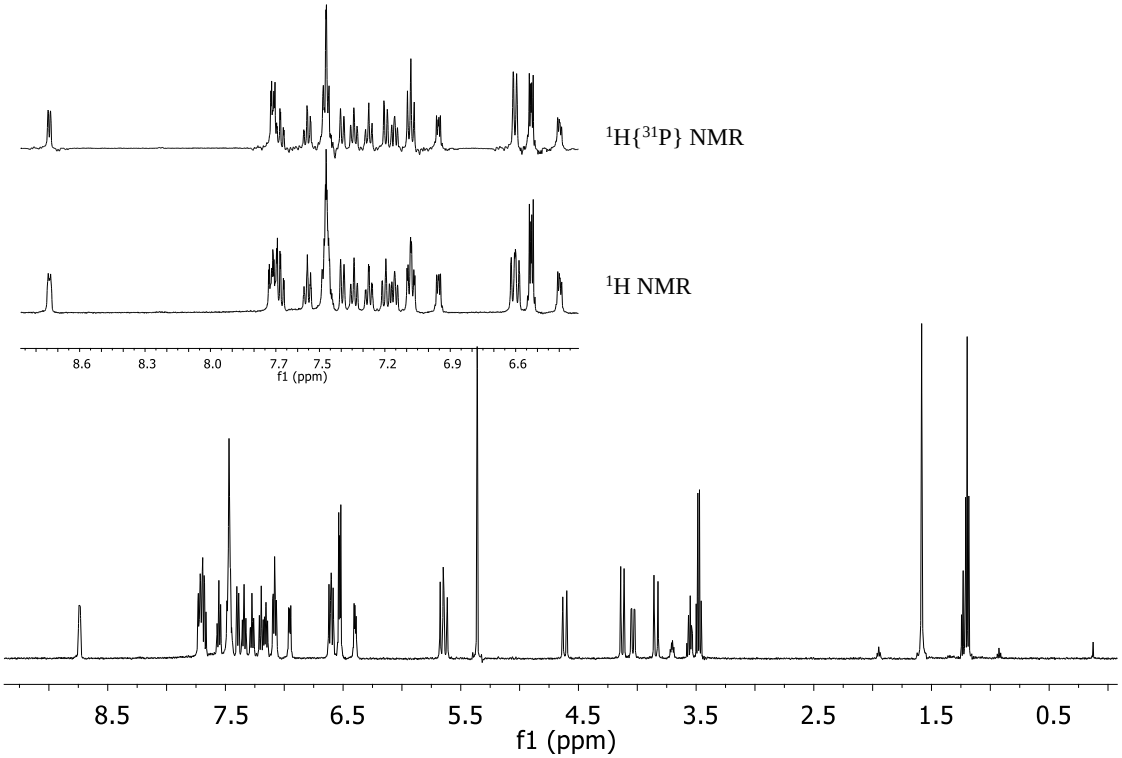

Figure SI3. $^{31}P\{^{1}H\}$ NMR (202.46 MHz, CD_2Cl_2, RT) of **11**

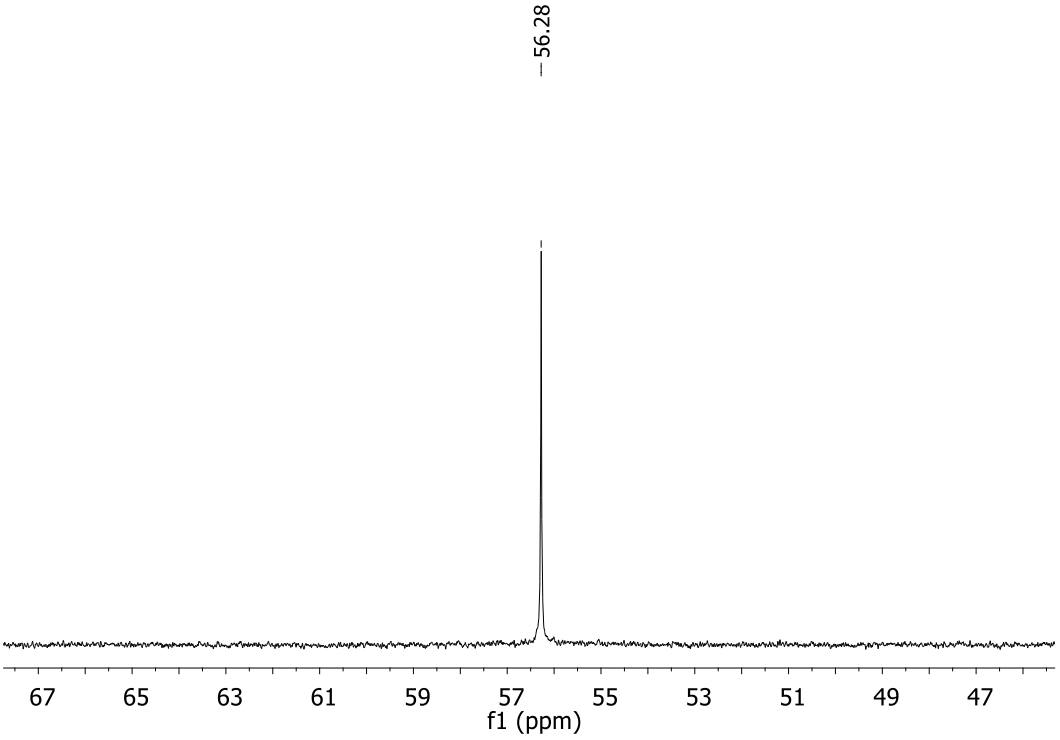

Figure SI4. $^{13}C\{^{1}H\}$ NMR (125.77 MHz, CD_2Cl_2, RT) of **11**

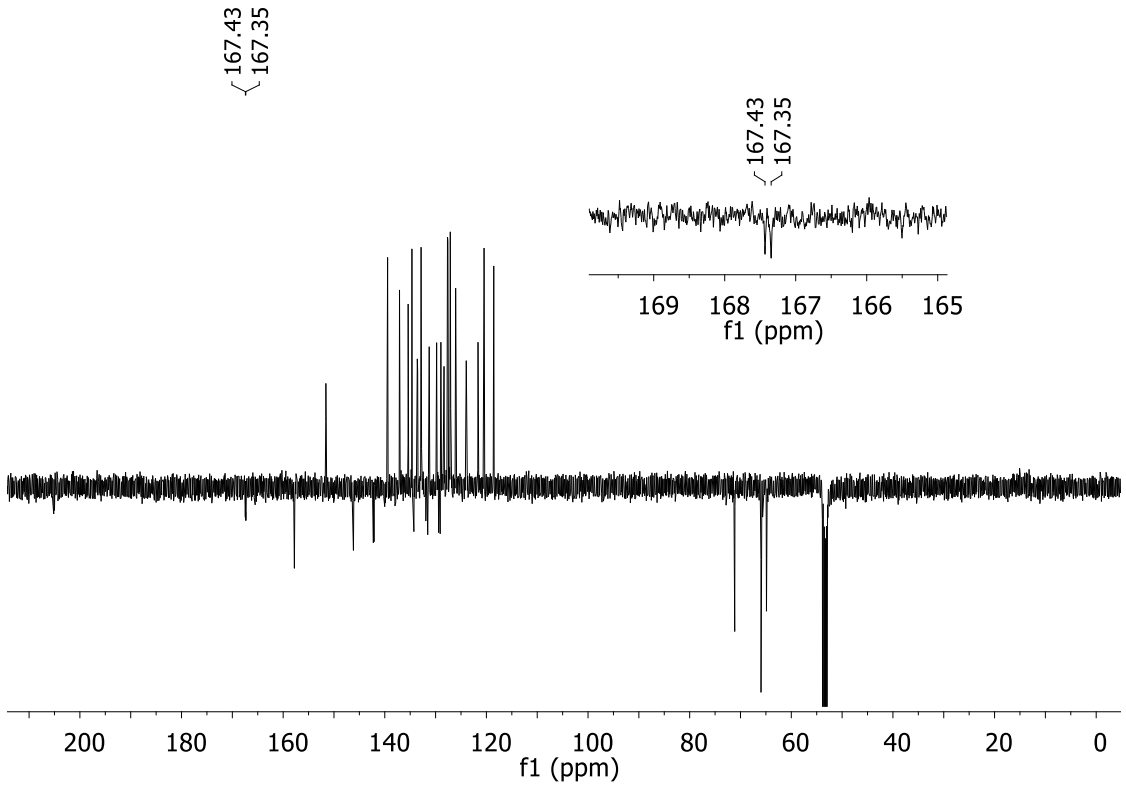

Figure SI5. ^{1}H-^{1}H COSY (CD_2Cl_2, RT) of **11**

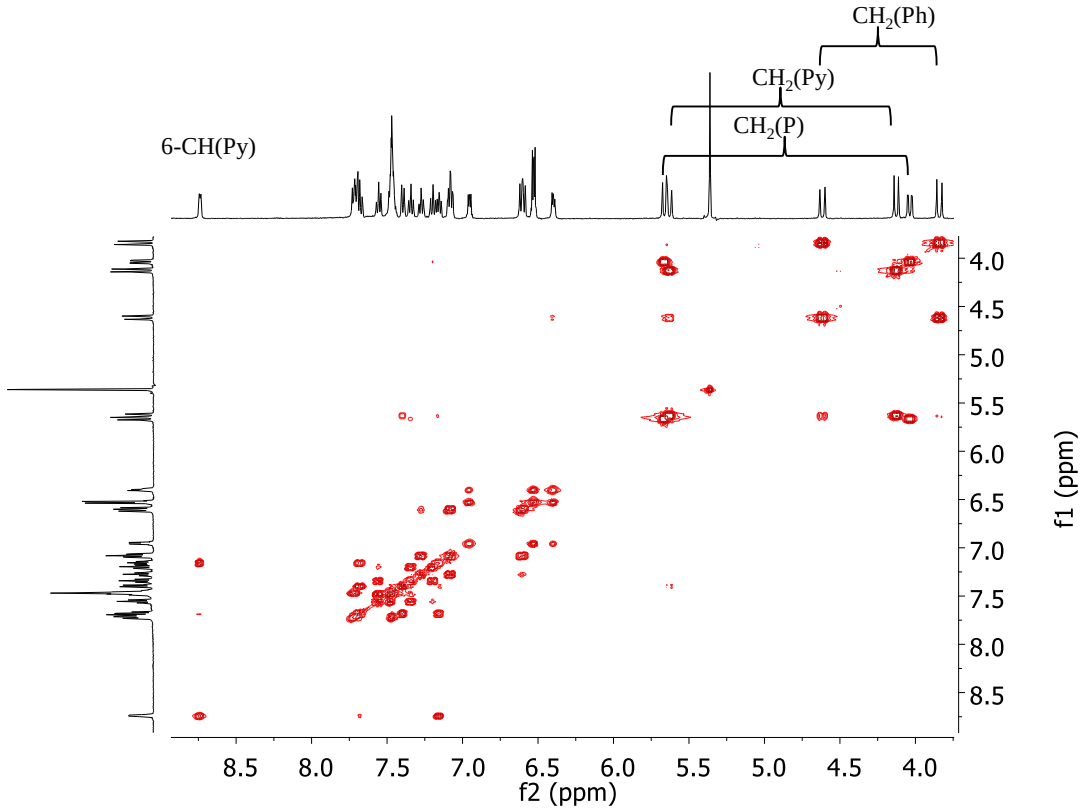

Figure SI6. ^{1}H-^{31}P HMBC (CD_2Cl_2, RT) of **11**

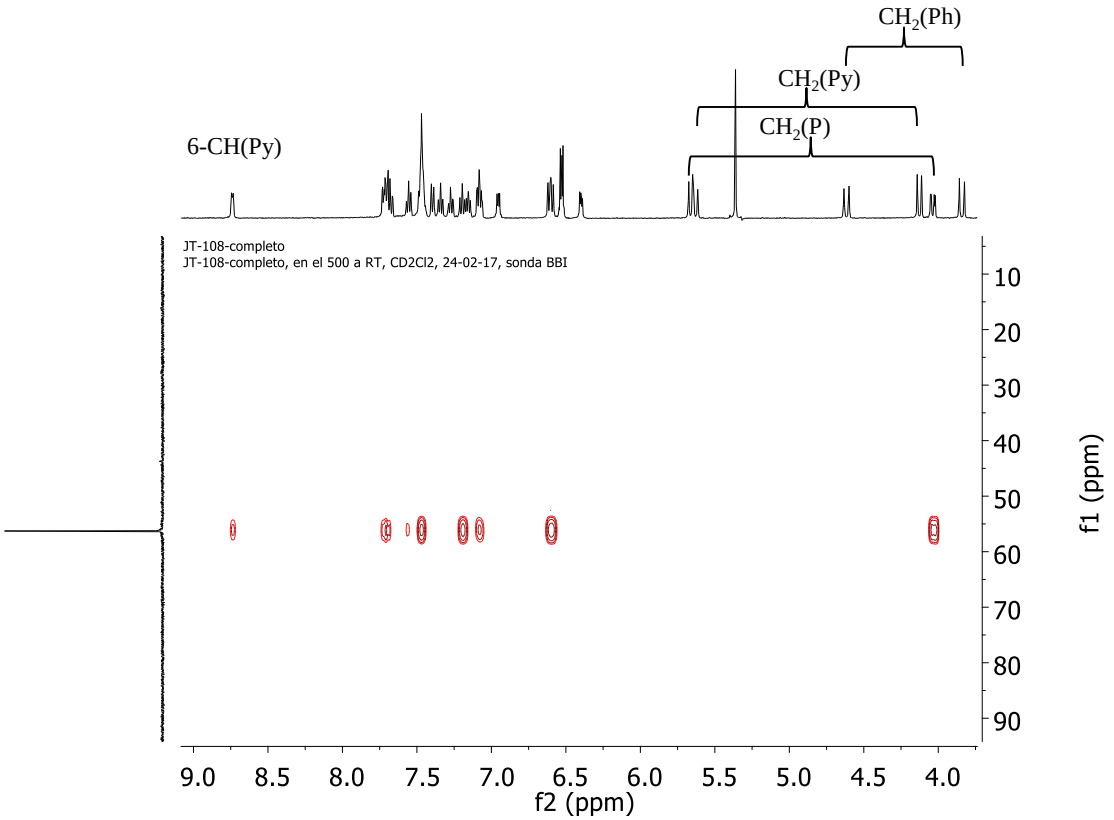

Figure SI7. ^{1}H-^{13}C HSQC (CD_2Cl_2, RT) of **11**

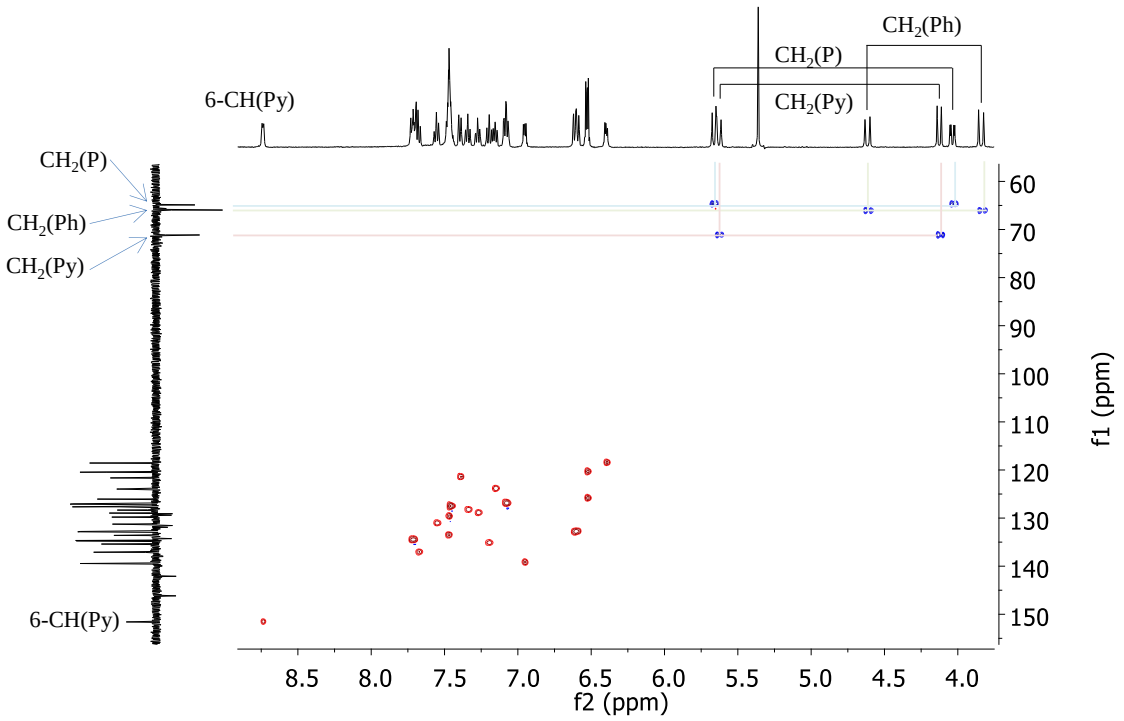

Figure SI8. ^{1}H-^{13}C HMBC (CD_2Cl_2, RT) of **11**

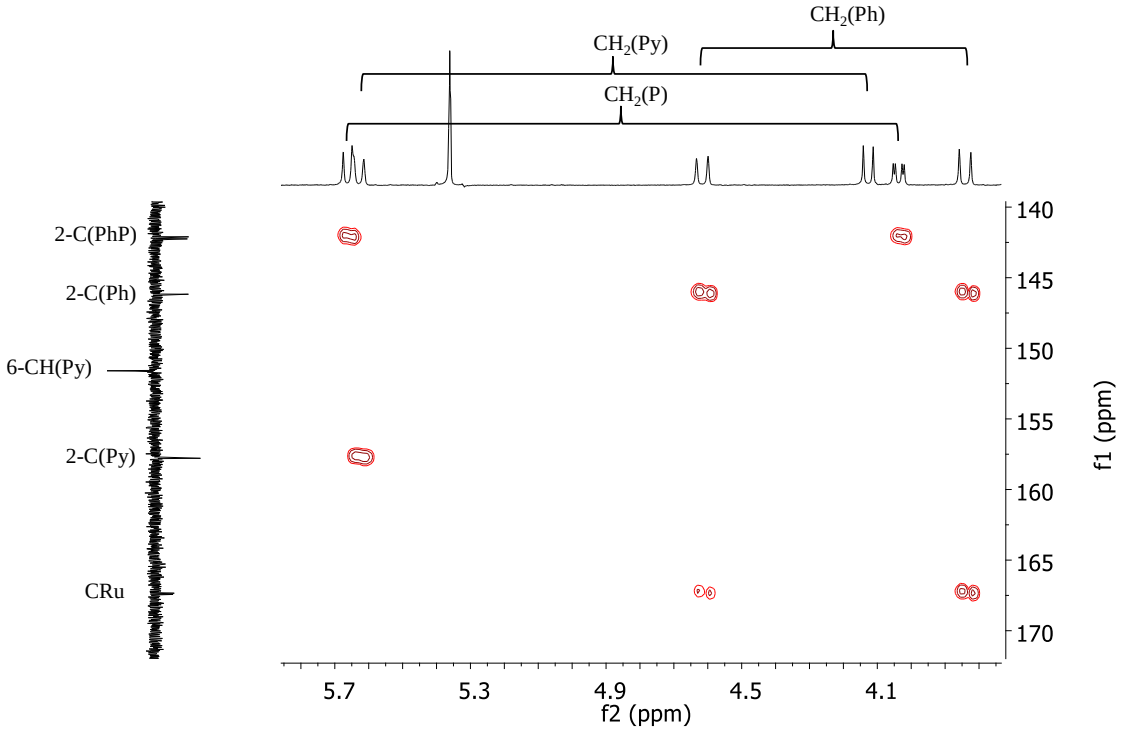

Chart SI1. Assignment of the methylene descriptors (A) and NOE relationship pattern (B) on (R_N)-*OC*-6-63-*C* isomers **11-13.**

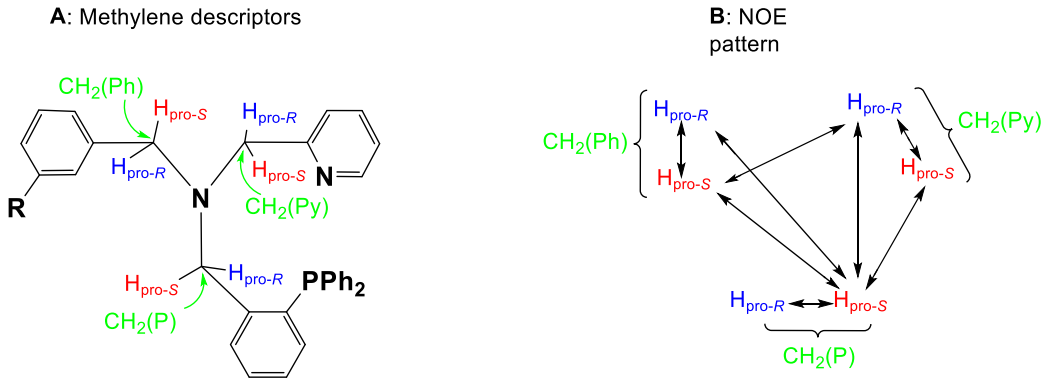

Figure SI9. ^{1}H-^{1}H NOESY (CD_2Cl_2, RT) of **11**

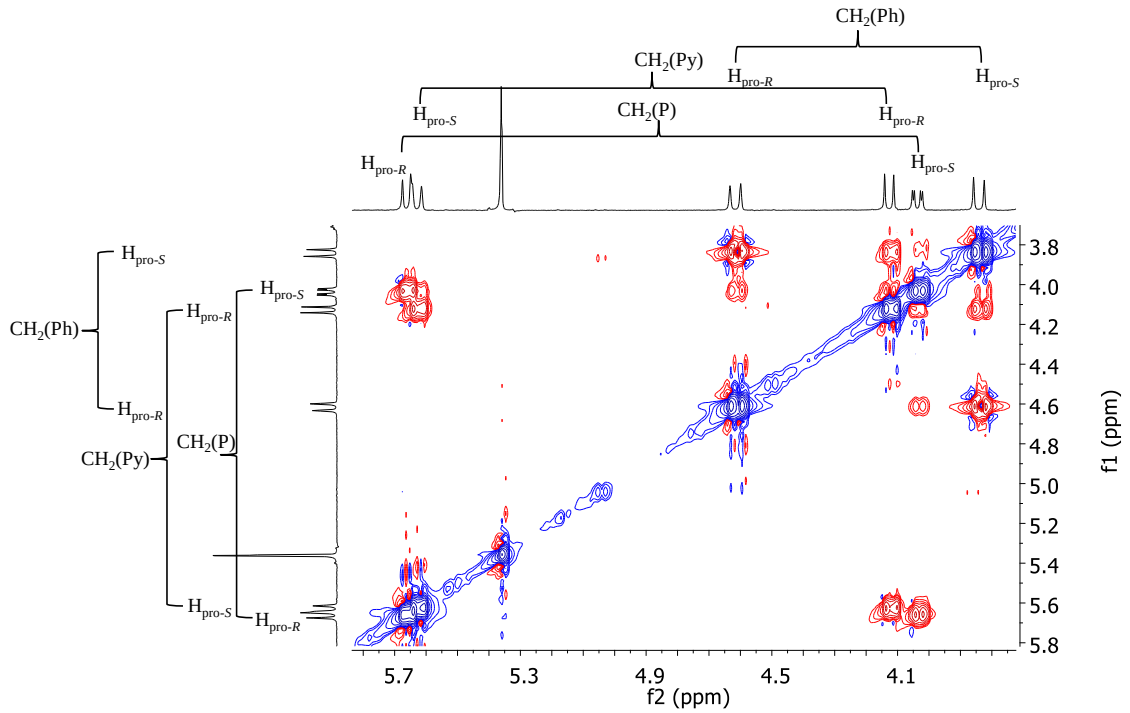

Figure SI10. ^{1}H NMR (500.13 MHz, CD_2Cl_2, RT) of **12**

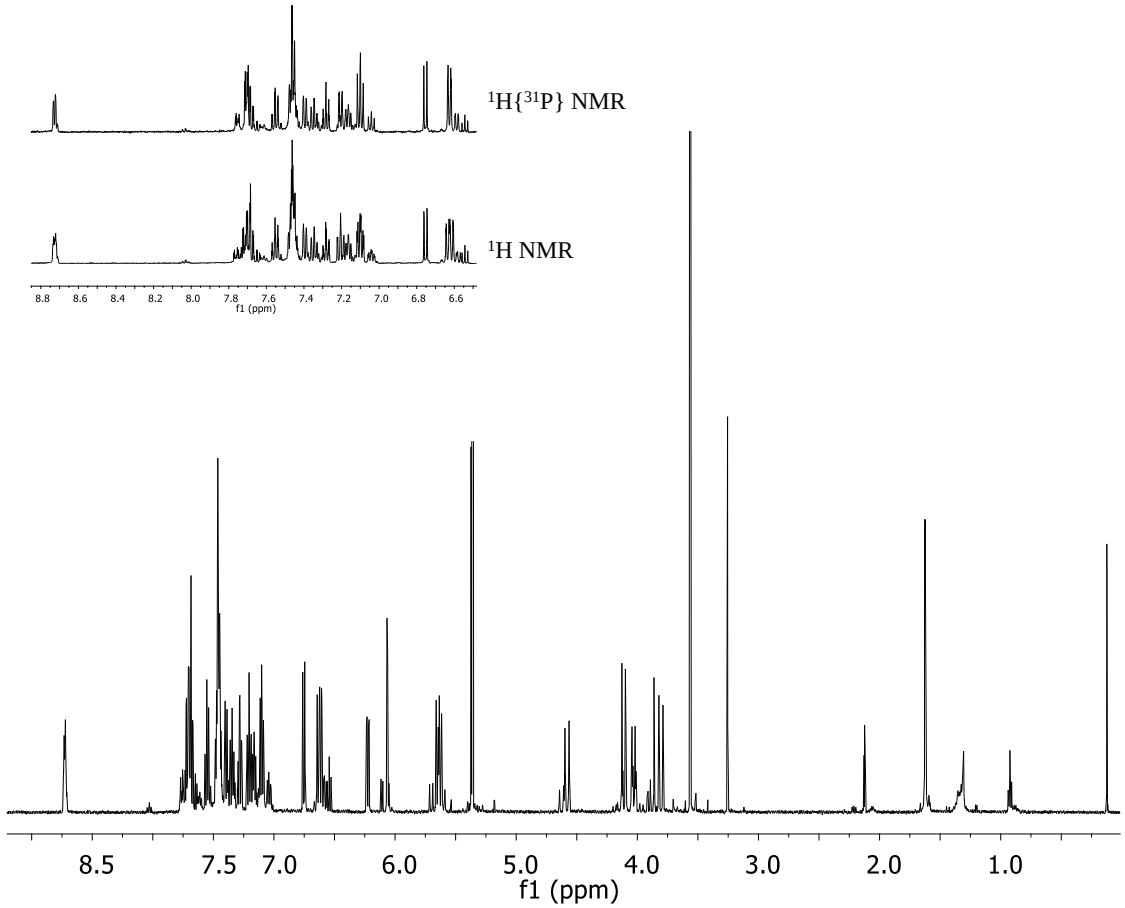

Figure SI11. $^{31}P\{^{1}H\}$ NMR (202.46 MHz, CD_2Cl_2, RT) of **12**

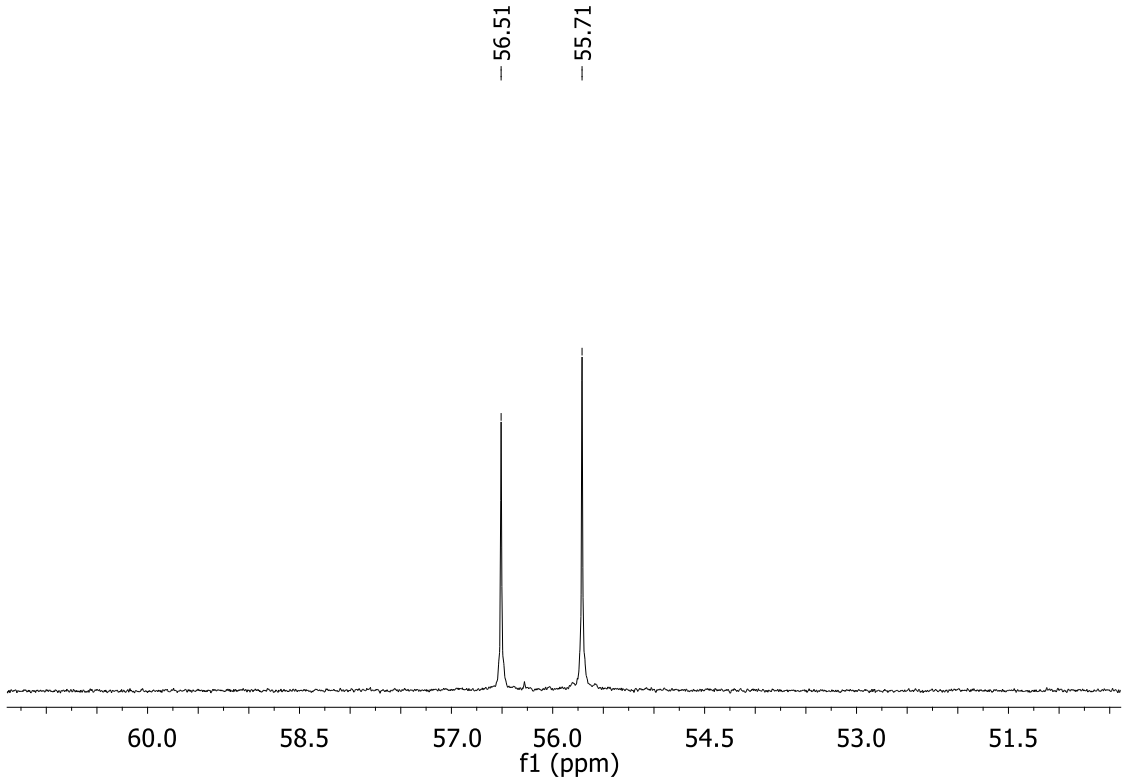

Figure SI12. $^{13}C\{^{1}H\}$ NMR (125.77 MHz, CD_2Cl_2, RT) of **12**

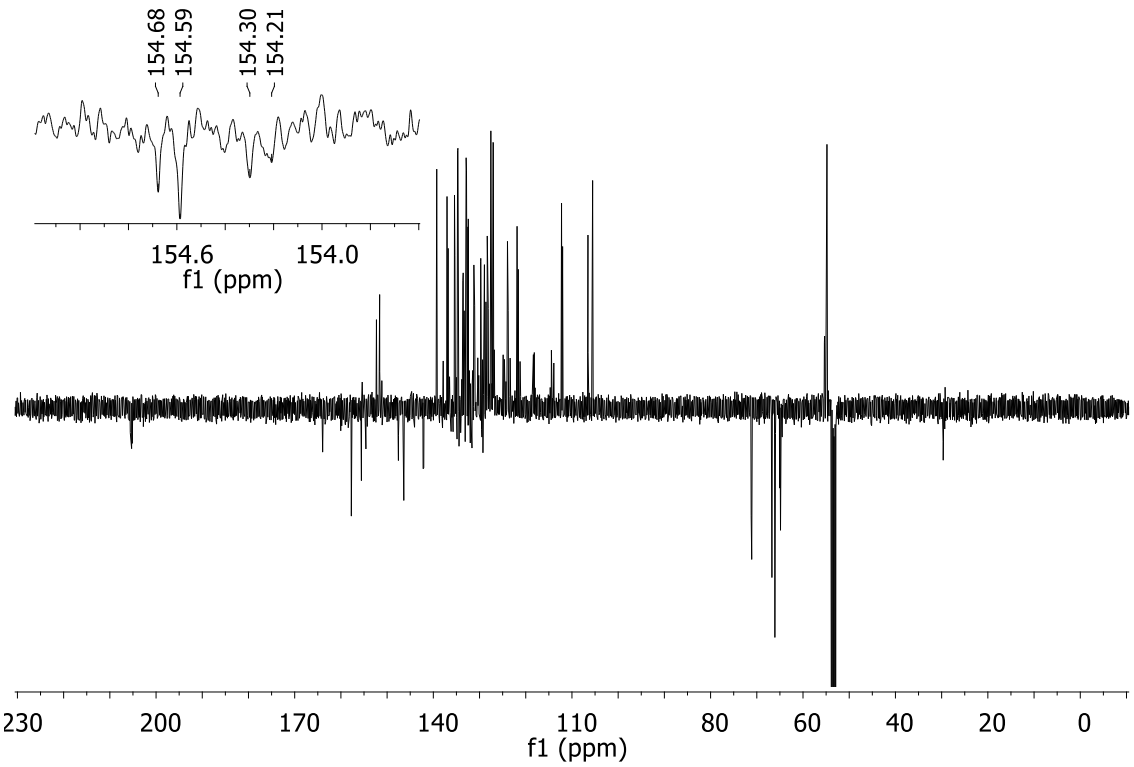

Figure SI13. ^{1}H NMR (500.13 MHz, CD_2Cl_2, RT) of **13**

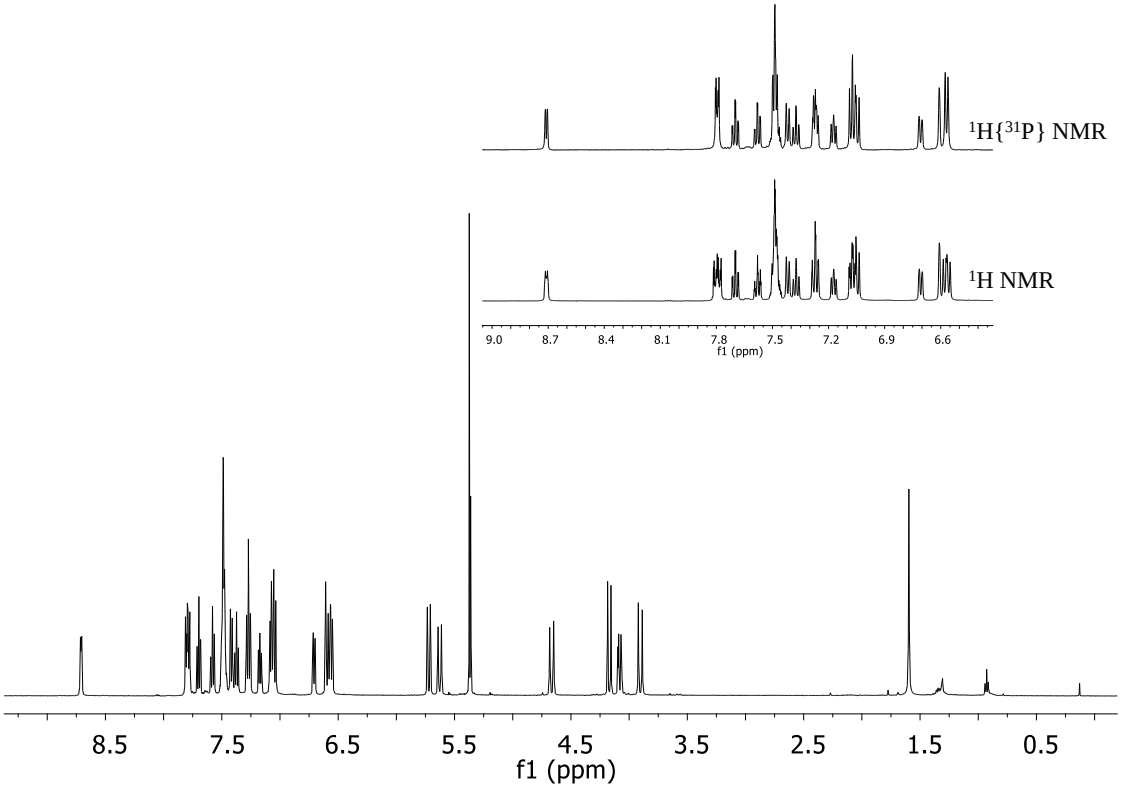

Figure SI14. $^{31}P\{^{1}H\}$ NMR (202.46 MHz, CD_2Cl_2, RT) of **13**

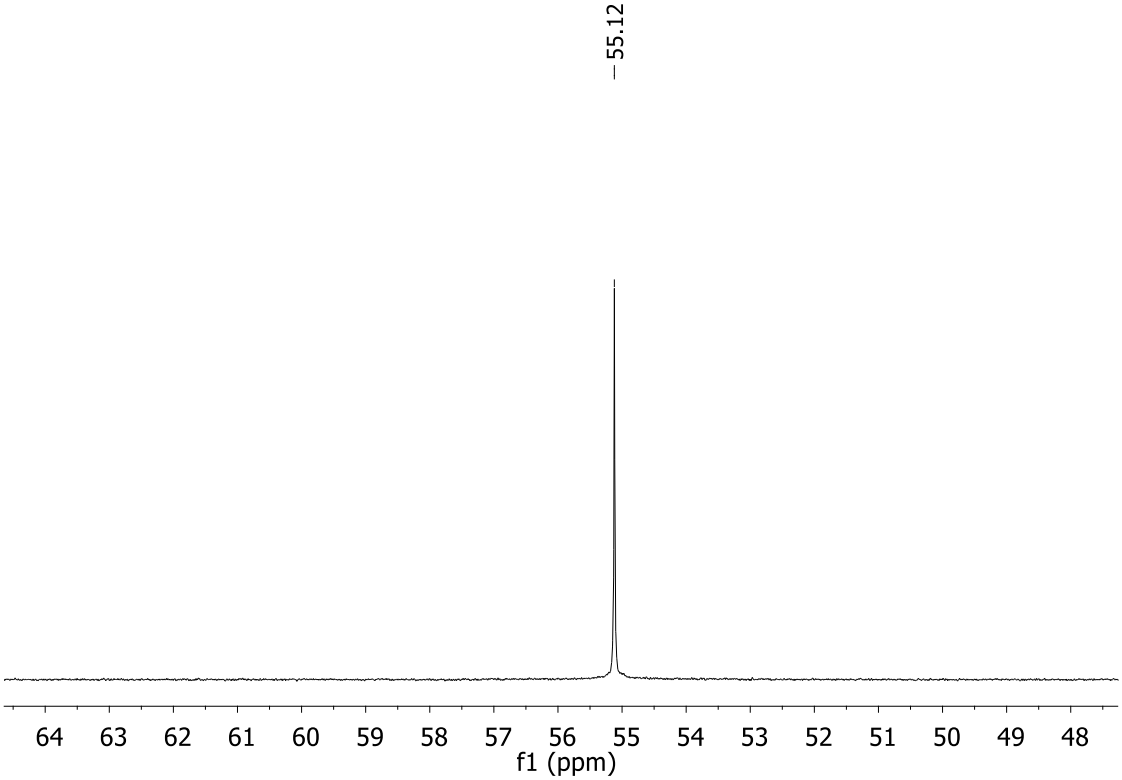

Figure SI15. $^{19}F\{^{1}H\}$ NMR (282.33 MHz, CD_2Cl_2, RT) of **13**

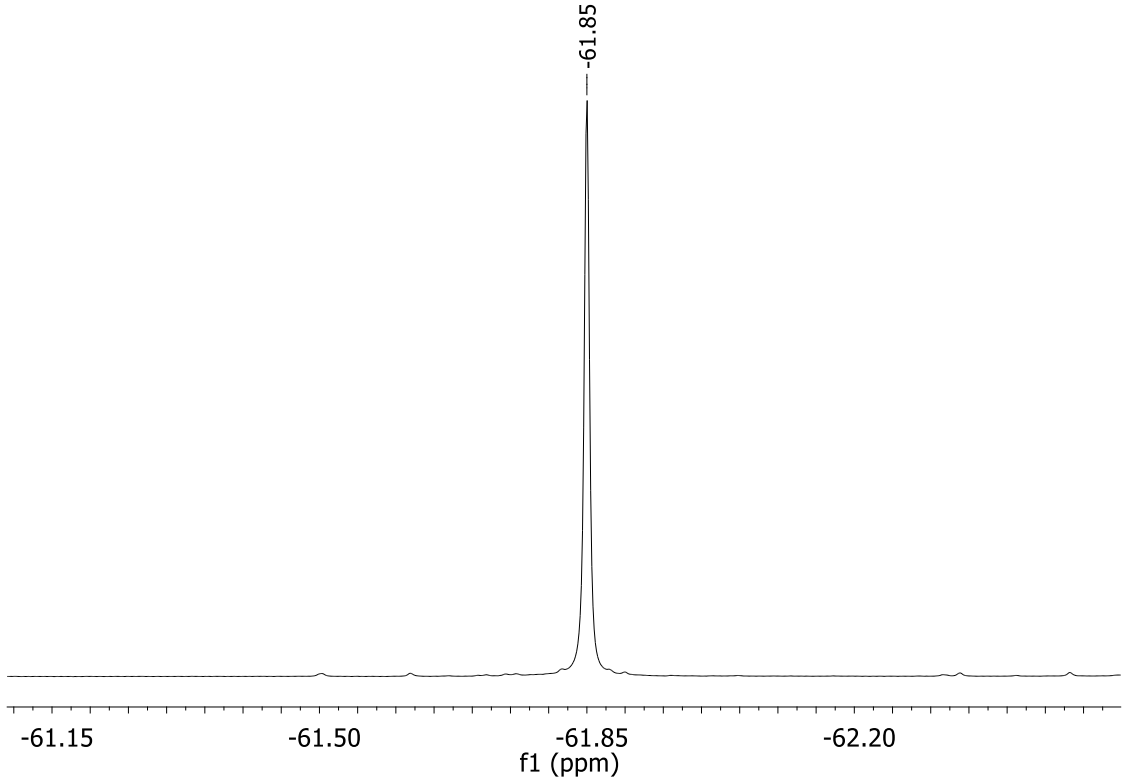

Figure SI16. $^{13}C\{^{1}H\}$ NMR (125.77 MHz, CD_2Cl_2, RT) of **13**

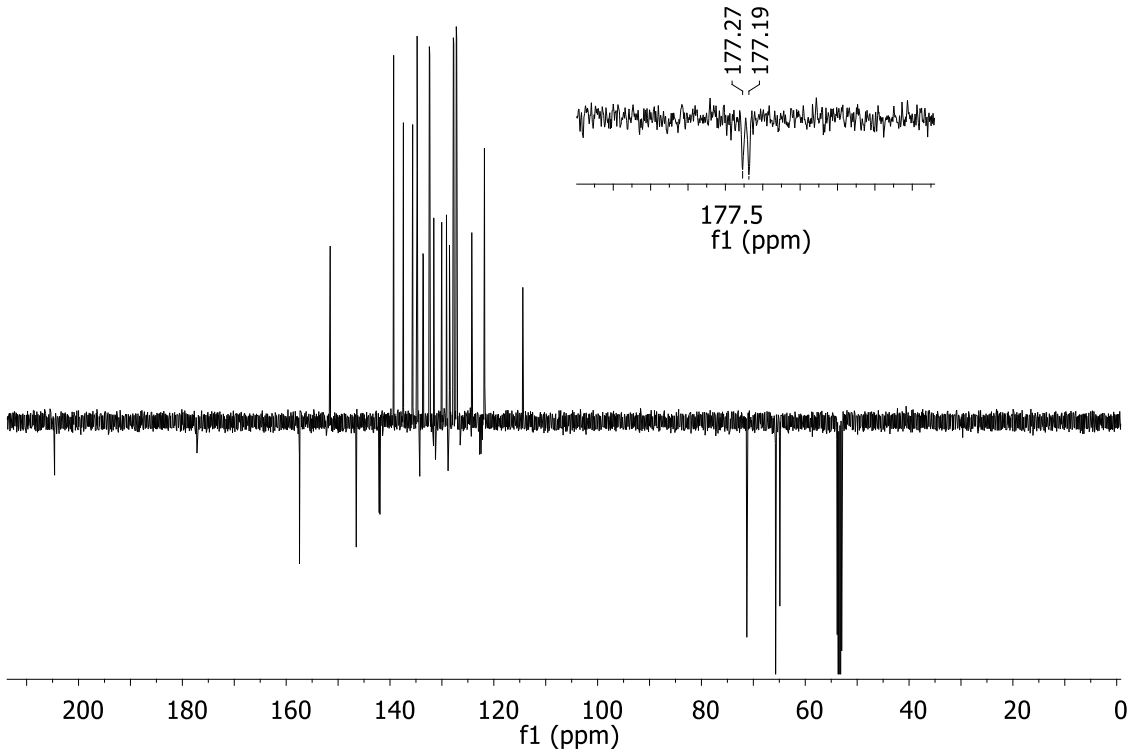

3. Crystal structure determination of complex 2

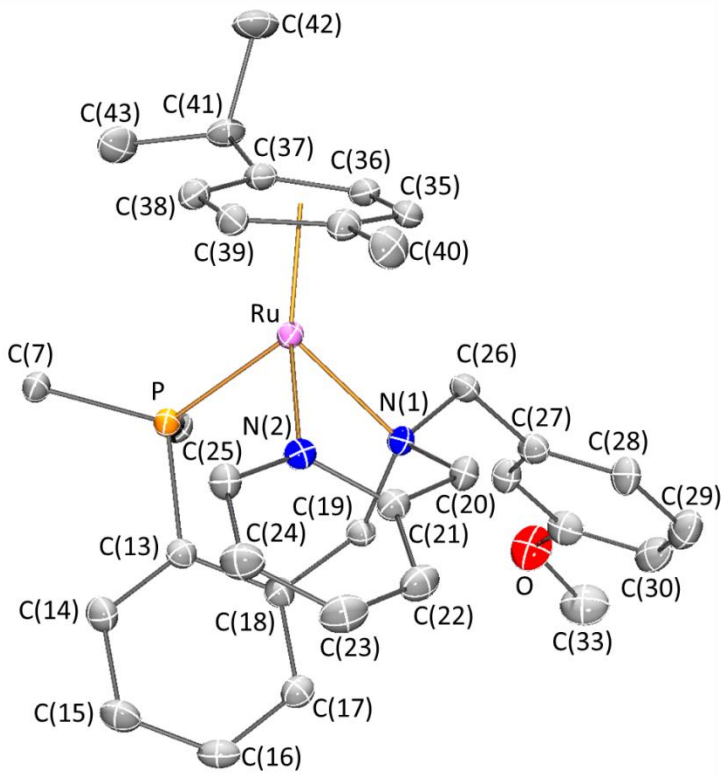

Figure SI17. Molecular structure of the cation of complex **2**. For clarity hydrogen atoms have been omitted and only *ipso* carbon atoms of PPh_2 group are depicted.

Table SI1. Selected bonds lengths (Å) and angles (º) for complex **2.**

Ru-P	2.3450(9)	P-Ru-N(2)	91.13(8)
Ru-N(1)	2.207(3)	P-Ru-Ct	130.93(1)
Ru-N(2)	2.097(3)	N(1)-Ru-N(2)	75.97(11)
Ru-Ct[a]	1.7642(1)	N(1)-Ru-Ct	131.11(1)
P-Ru-N(1)	87.90(8)	N(2)-Ru-Ct	122.68(1)

[a] Ct is the centroid of the ring of *p*-cymene ligand.

Crystal Data for 2: $C_{43}H_{45}F_{12}N_2OPRuSb_2 \cdot 2(CH_2Cl_2)$; M = 1379.20; yellow prism, 0.115 × 0.150 × 0.200 mm; triclinic *P-1*; a = 12.1011(5), b =14.0295(6), c = 15.7464(7) Å; α = 97.2940(10) °, β = 100.9750(10) °, γ=100.6920(10)°; V = 2542.09(19) Å^3; Z = 2; ρ_{calcd} = 1.802 g cm^{-3}; μ = 1.671 cm^{-1}; min. and max. transmission factors 0.6897 and 0.8264; $2\theta_{max}$ = 57.302°; 31030 reflections collected; 11854 unique reflections (R_{int} = 0.0235); number of data/restraints/parameters: 11854/4/609; final *GOF* = 1.103; R_1= 0.0400 [10454 reflections, $I > 2\sigma(I)$], *wR2* = 0.1102 for all data; largest difference peak:

2.588 e A^{-3}. Both dichloromethane solvent molecules have been found to be disordered. The disordered atoms have been included in the model in two positions with complementary occupancy factors and isotropically refined. Some geometrical restraints (in C-Cl bond lengths) and common isotropic atomic displacement parameter have been used for C and Cl atoms of the minor components. At the end of the refinement, highest residual density peaks are observed close to disordered chlorine atoms. Attempts to interpret them as an additional component of the disordered were unsuccessful.

4. Intermolecular interactions details of complex 5c

Table SI2. Geometrical parameters (Å, °) for hydrogen bond interaction between **5c** and **5c'**.

	D-H	H···A	D···A	D-H···A
C(20)-H(20)···O^{i}	0.99	2.70	3.514(4)	140

Symmetry code: i) *–x*, 1-*y*, 1-*z*.

Figure SI18. Adjacent **5c**/**5c**' molecules. A) Projection onto the methoxyphenyl fragment of **5c'**. b) Perspective view. Mean planes of methoxyphenyl fragment of **5c'** and **5c** are shown in green and red colours, respectively. Interplanar distance: 3.60 Å

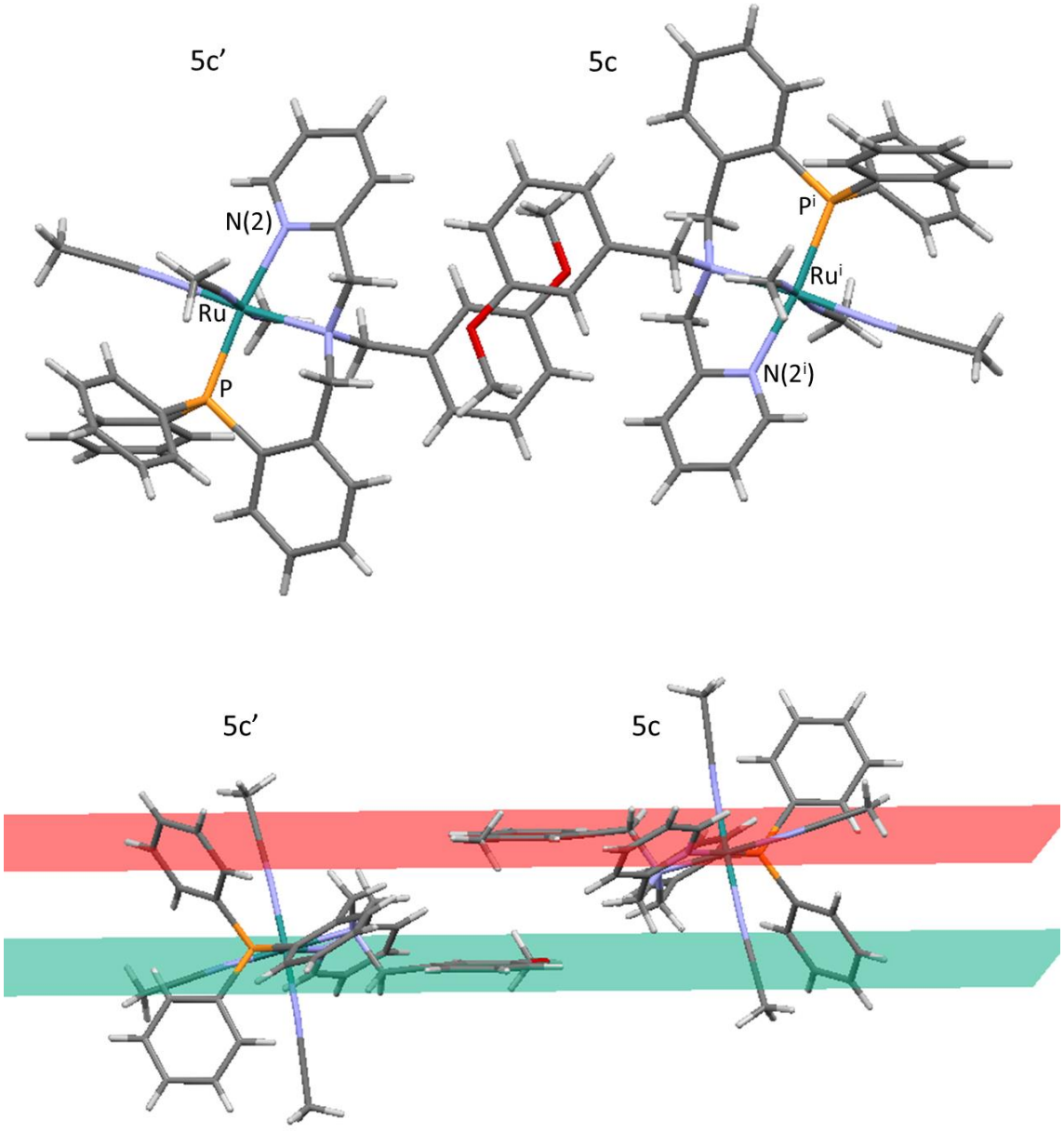

Symmetry code: i) *–x*, 1-*y*, 1-*z*.

5. Ring puckering parameters for complexes 1, 2, 5, 10a, 11, 12 and 13

Table SI3. Ring puckering parameters (Å, °) for complexes **1**, **2**, **5**, **10a**, **11**, **12** and **13**.

	1	**2**	**5c'**	**10a**	**11**	**12**	**13**
isomer	S_{Ru},R_N	S_{Ru},R_N	R_N	(S_N)-*OC*-6-25-*A*	(R_N)-*OC*-6-63-*C*	(R_N)-*OC*-6-63-*C*	(R_N)-*OC*-6-63-*C*
Ru-P-C(13)-C(18)-C(19)-N(1)							
q (Å)	0.9507(15)	0.950(2)	0.662(2)	0.7618(1)	0.6706(1)	0.6331(1)	0.681(3)
φ (º)	-137.26(13)	-137.2(2)	83.4(2)	-115.6(1)	-96.81(1)	-94.02(1)	-98.7(2)
θ (º)	102.53(12)	102.4(2)	101.7(2)	89.5(1)	75.30(1)	71.34(1)	77.53(17)
Conf.	$^2T_4$	$^2T_4$	$^6T_2$	$^{2,5}B$	$^5S_6$	$^5S_6$	$^5S_6$
Ru-N(1)-C(20)-C(21)-N(2)							
q (Å)	0.5720(18)	0.567(3)	0.481(3)	0.525(1)	0.4180(1)	0.4211(1)	0.442(3)
ϕ (º)	25.39(19)	25.6(3)	-142.4(3)	-145.2(2)	36.74(1)	37.40(1)	33.4(4)
conf	$^1T_2$ / E_2	$^1T_2$ / E_2	^2E	^2E	E_2	E_2	E_2
Ru-N(1)-C(26)-C(27)-C(28)							
q (Å)					0.0327(1)	0.0711(1)	0.111(3)
ϕ (º)					-106.1(1)	-117.14(4)	-90(2)
conf					E_3	$^2T_3$ / E_3	$^4T_3$